

PACS numbers: 02.50.Sk; 42.60.Lh; 42.55.Lt
DOI: 10.1070/QE2012v042n04ABEH014808

Simulation of the output power of copper bromide lasers by the MARS method

I.P. Iliev, D.S. Voynikova, S.G. Gocheva-Ilieva

Abstract. **The dependence of the output power of CuBr lasers (operating at wavelengths of 510.6 and 578.2 nm) on ten input physical parameters has been statistically analysed based on a large amount of experimental data accumulated for these lasers. Regression models have been built using the flexible nonparametric method of multivariate adaptive regression splines (MARS) to describe both linear and nonlinear local dependences. These models cover more than 97% initial data with an error comparable with the experimental error; they are applied to estimate and predict the output powers of both existing and future lasers. The advantage of the models constructed for estimating laser parameters over the standard parametric methods of multivariate factor and regression analysis is demonstrated.**

Keywords: *copper bromide laser, output laser power, multivariate adaptive regression splines, nonparametric model.*

1. Introduction

The subject of this study is copper bromide (CuBr) lasers, which generate at the wavelengths $\lambda_1 = 510.6$ nm and $\lambda_2 = 578.2$ nm. The lasers of these types are most efficient sources of visible light among metal vapour lasers. They are widely used in practice and are of great scientific interest [1].

These lasers have been intensively studied not only experimentally but also using methods of analytical and numerical simulation. The main results in this field have been obtained within kinetic models, which are generally based on several tens or even hundreds of interrelated differential equations describing the relationship of the physical processes occurring in the laser medium [1, 2]. At the same time, some new approaches to the study of these lasers have been developed in the last years; they are based on statistical treatment of accumulated experimental data with application of specialised computational methods and software [3–7]. These approaches directly yield important information about the main dependences of laser parameters and predict the behaviour of a specific laser system or a type of systems. Statistical methods make it also possible to reveal new relationships between the characteristics of the system under consideration that cannot be obtained by theoretical, numerical, and experimental studies.

The purpose of this study was to determine the explicit dependence of the output laser power on the main input parameters. To this end, we constructed nonparametric regression models by the method of multivariate adaptive regression splines (MARS) [8]. We used the MARS technique (1) to determine the dependences describing most adequately both locally linear and locally nonlinear terms; (2) to find the degree of influence of the input parameters on the output power; (3) to estimate the results of the known experiment, as well as to predict and plan new experiments; and (4) to compare the MARS results with those obtained by standard statistical methods. The study was performed on the basis of all existing experimental data on copper bromide lasers [9–17] that have been developed during the last several decades at the Laboratory of Metal Vapor Lasers of the Georgi Nadjakov Institute of Solid-State Physics, Bulgarian Academy of Sciences. Calculations were performed using the MARS software [18].

2. Description of data

We considered the following ten input laser variables (predictors): the inner diameter of the laser tube, D (mm); the inner diameter of the diaphragm, D_r (mm); the active-region length (the distance between the electrodes), L (cm); the supplied electric power, P_{in} (kW); the electric power per unit length (with allowance for 50% loss), $P_L = P_{in}/L$ (kW cm^{-1}); the electric pulse repetition frequency, P_{rf} (kHz); the buffer gas (neon) pressure, p_{Ne} (Torr); the additional gas (hydrogen) pressure, p_{H_2} (Torr); the equivalent capacitance of the capacitor battery, C (nF); and the temperature of the reservoir filled with CuBr, T_r (°C). The average output laser power P_{out} (W) will be considered as the main dependent variable.

We used the data for $n = 387$ experiments. The letter v will indicate the set of input variables in the following order: $v = (D, D_r, L, P_{in}, P_L, P_{rf}, p_{Ne}, p_{H_2}, C, T_r)$. For example, the maximum output power $P_{out} = 120$ W was obtained in the experiment characterised by $v_{387} = (58, 58, 200, 5, 12.5, 0.6, 17.5, 20, 1.3, 490)$ [14].

The basic statistical characteristics of the experiments are listed in Table 1. Note that on the whole they cannot be described by a multivariate normal distribution; therefore, the application of parametric methods to the complete sample used is not justified. However, this condition is not necessary for nonparametric methods (such as MARS), which have a wider range of application and are not related to a certain type of data distribution.

I.P. Iliev Department of Physics, Technical University of Plovdiv, 25 Tzanko Djusstabanov St, 4000 Plovdiv, Bulgaria; e-mail: iliev55@abv.bg;
D.S. Voynikova, S.G. Gocheva-Ilieva Department of Applied Mathematics and Modeling, Faculty of Mathematics and Informatics, Paisii Hilendarski University of Plovdiv, 24 Tzar Assen St., 4000 Plovdiv, Bulgaria

Received 28 December 2011
Kvantovaya Elektronika **42** (4) 298–303 (2012)
Translated by Yu.P. Sin'kov

Table 1. Statistical characteristics for a set of $n = 387$ measurements.

Variable	Minimum value	Maximum value	Mean value	Asymmetry	Excess
D	15.00	58.00	46.59 ± 10.072	–0.809 ± 0.12	1.451 ± 0.25
D_r	4.50	58.00	34.83 ± 18.31	0.265 ± 0.12	–1.602 ± 0.25
L	30.00	200.00	106.59 ± 70.70	0.478 ± 0.12	–1.670 ± 0.25
P_{in}	1.00	5.00	2.10 ± 1.27	1.065 ± 0.12	–0.321 ± 0.25
P_L	5.00	16.67	10.92 ± 2.51	–0.467 ± 0.12	0.183 ± 0.25
P_{rf}	3.20	125.50	23.24 ± 25.69	3.589 ± 0.12	11.530 ± 0.25
p_{Ne}	8.00	250.00	22.56 ± 24.17	6.389 ± 0.12	46.454 ± 0.25
p_{H_2}	0	0.80	0.36 ± 0.25	–0.416 ± 0.12	–1.430 ± 0.25
C	0.33	4.00	1.33 ± 0.61	2.313 ± 0.12	6.233 ± 0.25
T_r	350.00	590.00	478.22 ± 23.25	–1.673 ± 0.12	7.332 ± 0.25
P_{out}	0.25	120.00	34.024 ± 35.57	0.808 ± 0.12	–0.862 ± 0.25

3. MARS method

This method was developed by prominent American physicist and statistician J. Friedman in the 1990–1991 [8]. It is implemented in such program packages as MARS [18], STATISTICA, R, and some others. In the last decade, MARS has acquired a reputation of a predictive technique in different fields of science and technology [18, 19].

In comparison with other regression techniques, MARS models are more flexible and can approximate local nonlinearities of data. Within these models the predictors that affect most significantly the dependent variable are automatically selected, and the simulation results have a simple form and can easily be understood and interpreted. Both small and large data sets can be processed by the MARS method. Here, it is sufficient for approximation errors to be normally distributed. For statistically significant models the estimate bias is generally very small.

Suppose we have a data set $X = (x_1, x_2, ..., x_p)$ and a variable $y = y(X)$, which depends on these data. Let the variables y, x_1, x_2, ..., x_p be vectors of dimension n. The general expression for the MARS model $\hat{y}_{[M]}$ for approximating y has the form

$$\hat{y}_{[M]} = b_0 + \sum_{j=1}^{M} b_j F_j(X), \tag{1}$$

where b_0 and b_j are constant coefficients of the model ($j = 1, 2, ..., M$) and $F_j(X)$ are basis functions.

In the linear case the basis functions have the form of a one-dimensional mirror function:

$$F_j(X) = \max(0, x_k - c_k) \text{ or } F_j(X) = \max(c_k - x_k, 0). \tag{2}$$

Here, c_k is the constant (node) of a basis function with values lying in the domain of the variable x_k. Graphically, the linear MARS model is a partially linear function, which can be considered as a linear regression curve in each separate subinterval.

When constructing nonlinear MARS models, the basis functions can also contain products of two or more functions of type (2) with nonrepeating indices. For example, the basis function

$$F_j(X) = \max(0, x_k - c_k)\max(0, x_l - c_l) \tag{3}$$

can take into account the influence of the interaction between two predictors, x_k and x_l, on the dependent variable y. Note that the difference of MARS model (1) from the model of conventional splines is as follows: the nodes c_k, the real set of basis functions, and their number M are unknown beforehand and must be determined from a number of additional optimising conditions.

A model is constructed in two stages. First, some maximum number of possible basis functions (it will be denoted as M_0) and the maximum order of interaction between them (the number of terms in the products of basis functions) are specified. It is recommended to choose $M_0 \geqslant 3p$ [19]. The so-called step-by-step forward run is performed in the first stage. Beginning with some b_0 value (for example, $b_0 = \min_i y_i$), one pair of basis functions of type (2) is added to the model in each next step. For a current model with M basis functions, the variable, coefficients, and the corresponding desired variable node are determined from the condition for minimising the sum of squared errors,

$$S_{[M]} = \sum_{i=1}^{n} [y_i - \hat{y}_{[M]}(X_i)]^2.$$

If the forward run is finished after M_1 steps, one has M_1 embedded models. The second stage implies a backward run: step-by-step removal of the terms (one by one) that do not improve the model in the sense of its cross-validation [method of generated cross-validation (GCV)] [19, 20]. The best model with $m = M$ terms is chosen, for which a minimum is obtained for the quantity

$$\mathrm{GCV}_{[m]} = \frac{\sum_{i=1}^{n} [y_i - \hat{y}_{[m]}(X_i)]^2}{n[1 - c(m)/n]^2}, \quad m = 1, 2, ..., M_1, \tag{4}$$

where $c(m) = m + \delta(m - 1)/2$; $\delta \in [2, 3]$. The backward run makes it possible to exclude possible overfitting of the model. Note that, depending on the purposes of study, one can use each statistically obtained significant model.

4. MARS simulation of the output laser power

Based on the above-described data, we will construct different MARS models to estimate the output power P_{out} and obtain explicit expressions for the dependence of type (1). These models are built using all ten specified independent variables from Section 2 as predictors and the output power P_{out} as a dependent variable.

For simplicity we restrict ourselves to the results obtained with the aid of the best MARS models. Below any model will be denoted as $(M_0;r)$, where M_0 is the maximum number of initial basis functions and r corresponds to the chosen maximum order of interaction between predictors.

4.1. First-order best MARS models

First-order models are partially linear regression models (M_0;1) for each of the basis functions of model (1). Let us consider the model (30;1) in detail. The best MARS model contains the following 18 basis functions:

$$
\begin{aligned}
&F_1 = \max(0, P_{\text{in}} - 2.5), \quad F_3 = \max(0, C - 1.9),\\
&F_5 = \max(0, D_{\text{r}} - 40), \quad F_6 = \max(0, 40 - D_{\text{r}}),\\
&F_7 = \max(0, C - 2.18), \quad F_9 = \max(0, C - 1.3),\\
&F_{11} = \max(0, P_{\text{rf}} - 16.3), \quad F_{13} = \max(0, P_{\text{rf}} - 21.5),\\
&F_{15} = \max(0, C - 1.1), \quad F_{17} = \max(0, C - 1),\\
&F_{19} = \max(0, P_{\text{rf}} - 18.5), \quad F_{21} = \max(0, P_{\text{in}} - 2),\\
&F_{23} = \max(0, P_{\text{rf}} - 26), \quad F_{25} = \max(0, P_L - 10),\\
&F_{26} = \max(0, 10 - P_L), \quad F_{27} = \max(0, p_{\text{H}_2} - 0.5),\\
&F_{28} = \max(0, 0.5 - p_{\text{H}_2}), \quad F_{29} = \max(0, P_{\text{rf}} - 14).
\end{aligned}
\tag{5}
$$

The corresponding MARS model for the output power P_{out} has the form

$$
\begin{aligned}
P_{\text{out}}^{(30;1)} &= 31.6223 - 28.9857F_1 + 120.663F_3\\
&+ 1.10983F_5 - 0.436723F_6 - 78.8721F_7\\
&- 112.399F_9 - 3.25176F_{11} + 8.49341F_{13}\\
&+ 209.183F_{15} - 142.364F_{17} - 6.14717F_{19}\\
&+ 44.4853F_{21} - 2.54973F_{23} - 1.63555F_{25}\\
&- 1.60555F_{26} - 34.5407F_{27} - 9.7688F_{28}\\
&+ 3.45331F_{29}.
\end{aligned}
\tag{6}
$$

In formulas (5) and (6), only six of ten input variables affect significantly the model: C (100), P_{in} (78.3), P_{rf} (63.9), D_{r} (43.5), P_{L} (14.6), and p_{H_2} (13.0) (their relative contributions are given in parentheses). One can easily find the individual contribution of each predictor by equating to zero all the model terms that do not contain this predictor. As an example Fig. 1 shows the contributions of the predictors P_{in} and C. It can be seen that a change in P_{in} does not affect the model in the interval [1, 2], whereas in the interval [2, 2.5] its contribution amounts to 0–25 and in the interval [2.5, 5] the contribution gradually increases and reaches 65. Similarly, one can easily estimate the influence of the capacitance C and each predictor on the model.

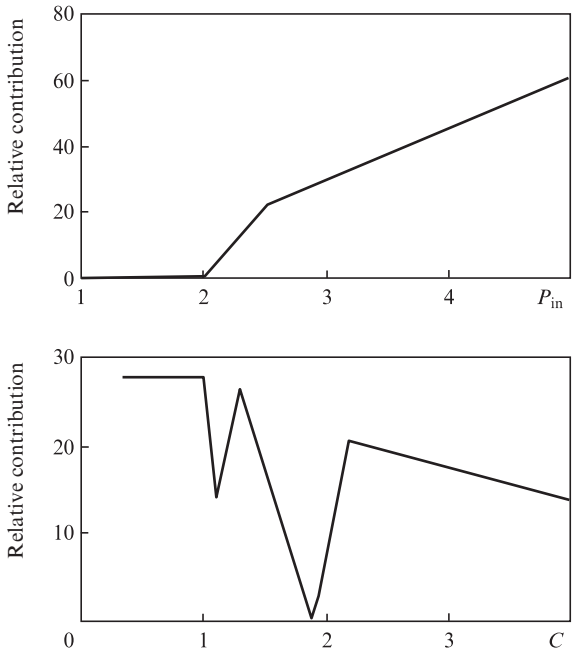

Figure 1. Contributions (in normalised units) of the input power P_{in} and the capacitor battery capacitance C to model (5), (6).

Model (5), (6) describes 98% of all data with a statistical significance $P = 0$ and a significance of the coefficients in (6) less than 0.00128. The model is very easy to use for calculating the predicted value $P_{\text{out}}^{(30;1)}$ if the predictor values are set. For example, for the set v = (40, 40, 120, 2.6, 10.83, 0.6, 17.5, 20, 1, 450), we first find from (5) that $F_1 = 0.1$, $F_3 = F_5 = F_6 = F_7 = F_9 = 0$, $F_{11} = 1.2$, $F_{13} = F_{15} = F_{17} = F_{19} = 0$, $F_{21} = 0.6$, $F_{23} = 0$, $F_{25} = 0.83$, $F_{26} = 0$, $F_{27} = 0.1$, $F_{28} = 0$, and $F_{29} = 3.5$. Then, substituting these values into (6), we obtain $P_{\text{out}}^{(30;1)}(v) = 58.78$ W. The experimental value for this measurement is 57.8 W.

The results obtained for the main first-order models are listed in Table 2. These models are constructed for subsequent comparison with higher-order models of interaction between predictors.

Table 2. Main characteristics of the best MARS models for calculating the output power P_{out}. The predictors are given in descending order with respect to their relative contributions to the models.

r	M_0	R^2	G_{R^2}	Standard regression error	Number of predictors	M	Predictors
1	20	0.9744	0.9700	5.60	4	13	P_{in}, C, P_{rf}, D_{r}
	25	0.9786	0.9737	5.31	5	15	P_{in}, C, P_{rf}, D_{r}, D
	30	0.9816	0.9765	4.95	6	18	C, P_{in}, P_{rf}, D_{r}, P_L, p_{H_2}
	35	0.9818	0.9763	4.93	6	19	C, P_{in}, P_{rf}, D_{r}, p_{H_2}, P_L
	40	0.9818	0.9762	4.92	6	19	C, P_{in}, P_{rf}, D_{r}, p_{H_2}, P_L
2	20	0.9856	0.9817	4.35	6	15	P_{in}, C, P_{rf}, L, p_{H_2}, P_L
	25	0.9885	0.9851	3.9	6	17	P_{in}, C, P_{rf}, D_{r}, P_L, p_{H_2}
	30	0.9910	0.9874	3.48	6	21	P_{in}, C, P_{rf}, D_{r}, p_{H_2}, P_L
	35	0.9944	0.9918	2.74	6	25	P_{in}, C, P_{rf}, D_{r}, p_{H_2}, P_L
	40	0.9950	0.9923	2.51	7	26	P_{in}, C, P_{rf}, D_{r}, p_{H_2}, P_L, D_{r}
3	20	0.9872	0.9838	4.11	6	16	P_{in}, C, P_{rf}, P_L, p_{H_2}, L
	25	0.9904	0.9879	3.55	6	16	P_{in}, C, P_{rf}, P_L, p_{H_2}, L
	30	0.9921	0.9888	3.26	7	22	P_{in}, C, P_{rf}, P_L, p_{H_2}, L, D_{r}
	35	0.9934	0.9894	3.00	8	28	P_{in}, C, P_{rf}, P_L, p_{H_2}, L, D_{r}, p_{Ne}
	40	0.9945	0.9903	2.71	8	31	P_{in}, C, P_{rf}, P_L, p_{H_2}, L, D_{r}, T_{r}

4.2. Second-order best MARS models

There are not only linear but also nonlinear local dependences between predictors. Therefore, we will construct second-order interaction models [see formula (3)]. Let us consider model (30;2) as an example. It is built using the following 22 basis functions:

$$
\begin{aligned}
&F_1 = \max(0, P_{\text{in}} - 2.5), && F_2 = \max(0, 2.5 - P_{\text{in}}),\\
&F_3 = \max(0, C - 0.33)F_1, && F_4 = \max(0, P_{\text{rf}} - 17.5)F_1,\\
&F_5 = \max(0, 17.5 - P_{\text{rf}})F_1, && F_7 = \max(0, 0.6 - p_{\text{H}_2}),\\
&F_8 = \max(0, P_{\text{rf}} - 23)F_2, && F_{10} = \max(0, P_L - 7.5)F_2,\\
&F_{11} = \max(0, 7.5 - P_L)F_2, && F_{12} = \max(0, P_L - 9.58333)F_2,\\
&F_{14} = \max(0, P_{\text{rf}} - 16)F_1, && F_{16} = \max(0, P_{\text{rf}} - 18.5)F_1,\\
&F_{19} = \max(0, 1.9 - C), && F_{20} = \max(0, P_L - 7.5)F_{19},\\
&F_{21} = \max(0, 7.5 - P_L)F_{19}, && F_{22} = \max(0, D_{\text{r}} - 20)F_{19},\\
&F_{23} = \max(0, 20 - D_{\text{r}})F_{19}, && F_{24} = \max(0, p_{\text{H}_2} - 0.3)F_{19},\\
&F_{25} = \max(0, 0.3 - p_{\text{H}_2})F_{19}, && F_{26} = \max(0, P_{\text{in}} - 2)F_{19},\\
&F_{28} = \max(0, C - 1.3)F_1, && F_{30} = \max(0, P_L - 5)F_1.
\end{aligned}
\tag{7}
$$

The corresponding model for P_{out} contains 21 functions from set (7) and has the form

$$
\begin{aligned}
P_{\text{out}}^{(30;2)} &= 35.0442 - 44.6739F_1 - 26.0407F_2\\
&+ 68.9544F_3 + 6.30534F_4 - 5.30336F_5\\
&- 25.2627F_7 - 0.0240315F_8 + 10.1025F_{10}\\
&+ 14.1118F_{11} - 12.0007F_{12} - 5.37771F_{14}\\
&- 7.34248F_{16} - 0.850553F_{20} - 9.95073F_{21}\\
&+ 1.15859F_{22} + 0.928972F_{23} - 48.494F_{24}\\
&+ 21.027F_{25} + 34.1073F_{26} - 35.9377F_{28}\\
&- 1.4502F_{30}.
\end{aligned}
\tag{8}
$$

Model (7),(8) contains six of ten initial predictors. In descending order with respect to the influence on the model, these are the following variables (with their relative contributions in parentheses): P_{in} (100), C (38), P_{rf} (30), D_{r} (15), p_{H_2} (12), and P_{L} (10). Partial second-order interaction (also in descending order with respect to their relative contributions to the model) was found for the following groups of variables: $\{P_{\text{in}}, P_{\text{rf}}\}$, $\{P_{\text{in}}, C\}$, $\{P_{\text{in}}, p_{\text{H}_2}\}$, $\{P_{\text{in}}, P_L\}$, $\{D_{\text{r}}, C\}$, $\{C, p_{\text{H}_2}\}$, and $\{P_L, C\}$. The contribution regions for the first two of these groups are shown in Fig. 2. To increase the output power, one must determine the ranges of values in which individual predictors should be chosen. For example, it can be seen in Fig. 2a that the influence of the group $\{P_{\text{in}}, P_{\text{rf}}\}$ reaches a maximum in the intervals $P_{\text{rf}} \in [50, 125]$ and $P_{\text{in}} \in [2.5, 3.5]$. Similarly, Fig. 2b shows that the influence of the group $\{P_{\text{in}}, C\}$ on the output power is maximum at $P_{\text{in}} \in [4.5, 5]$ and $C \in [1.6, 2]$.

Model (7),(8) describes 99% of all data with a statistical significance $P = 0$ and significance coefficients in (8) smaller than 0.00201.The results obtained for the main second-order models are also listed in Table 2.

We also constructed third- and higher order models; however, as can be seen in Table 2, they did not radically improve the results in comparison with the second-order models.

5. Comparison of models

Models can be compared in their main parameters (see Table 2). According to Table 2, the determination coefficient for linear models is $R^2 = 97\%$–98%, while for the other models $R^2 > 99\%$ (this parameter characterises the percentage of the observations described by a given model). The cross-validation coefficient R^2 for G_{R^2} is also rather large [20]. This means the following: if one constructs a model based on a 90% random 'learning' data sample and uses it to predict the rest 10% data, the degree of approximation (in percent) will be G_{R^2}.

Among all models, it is the second- and the third-order interaction models that describe most adequately locally linear and locally nonlinear terms. For example, it is sufficient to choose 30 or 40 initial functions and models (30;2), (30;3) or (40;2), (40;3). These models give an approximation error of about 5%, which is comparable with the experimental error.

The last column of Table 2 shows that an increase in the model order and in the number M_0 of initial basis functions stabilises the set of significant predictors. For example, the variables P_{in}, C, P_{rf}, D_{r}, p_{H_2}, and P_L are significant when determining the output power P_{out}. Note that the relative contribution of D_{r}, p_{Ne}, and T_{r} in models (40;2), (30;3), (35;3), and (40;3) is less than 4, and their influence can be neglected.

Our previous statistical studies using parametric methods of multivariate factor and regression analyses led to models

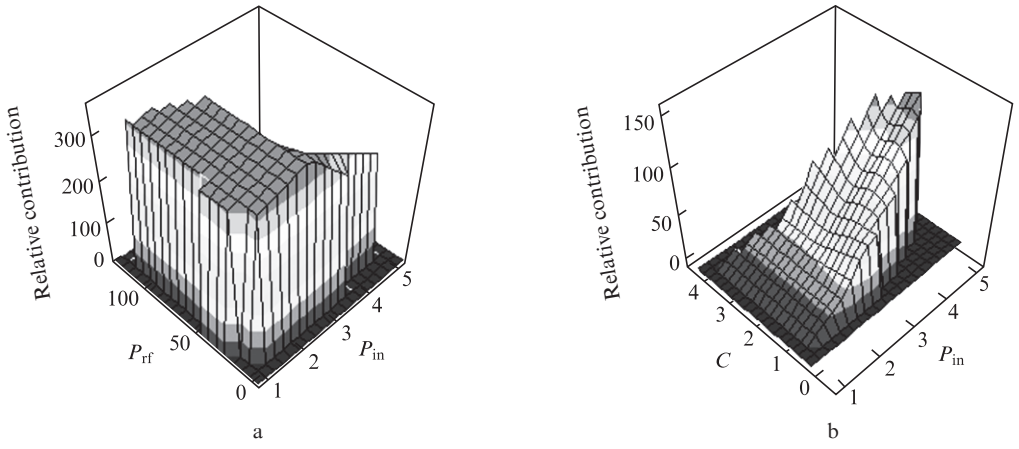

Figure 2. Contributions (in normalised units) of the interaction between (a) P_{in} and P_{rf} and (b) P_{in} and C to model (7),(8).

based on random samples from the data set under consideration. Based on the variables from the set P_{in}, D_r, D, L, P_L, p_{H_2}, linear, nonlinear parametric, and MARS models were developed for the output power in [3], [6], and [5], respectively. Note also that the variables C and P_{rf} are not used in these models, because they take only several optimised values, and this factor is disregarded in parametric methods. These models had worse statistical characteristics and a more limited range of application than the MARS model constructed by us. This is related, on the one hand, to strict limitations on the application of parametric methods, and, on the other hand, to the presence of partially nonlinear dependences and high multicollinearity of the data analysed for copper bromide lasers.

6. Estimation and prediction of experimental results using MARS models

We will apply MARS models to predict the results of known and future experiments. As was shown in Subsection 4.1, having some model and a set of its parameters, one can easily calculate the values of the basis functions and obtain the corresponding estimate for P_{out}. For definiteness, we will use the best MARS models: (30;2), (40;2), (30;3), and (40;3).

6.1. Prediction of the results of known experiments

Model (30;2) yields the following estimate for the experiment with the set of input parameters v_{387} and $P_{out} = 120$ W:

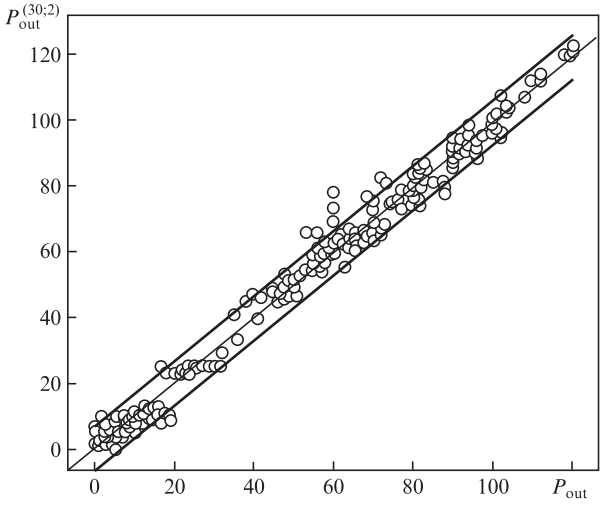

Figure 3. Approximation of the output power P_{out} using the best MARS model (30;2). The solid lines show the 5% deviation from the mean value.

$P_{out}^{(30;2)} = 119.7$ W. The experimental P_{out} values are compared with their model estimates by formulas (7), (8) in Fig. 3.

To demonstrate the possibilities of predicting known output powers based on 377 experiments, we constructed four models: (30;2), (40;2), (30;3), and (40;3) and predicted, based on them, the data of the last ten of 387 experiments. These results are listed in Table 3 in ascending order with respect to P_{out}.

Table 3. Results predicted based on 377 observations, using four MARS models for ten experiments ($D = 58$ mm, $D_r = 58$ mm, $L = 200$ cm, $p_{H_2} = 0.6$ Torr, $p_{Ne} = 20$ Torr, $C = 1.3$ nF, $T_r = 490$ °C).

n	P_{in}	P_L	P_{rf}	P_{out}^{exp}	$P_{out}^{(30;2)}$	$P_{out}^{(40;2)}$	$P_{out}^{(30;3)}$	$P_{out}^{(40;3)}$
378	4	10.00	18.5	104	104.1	104.2	103.4	105.7
379	5	12.50	15	106	106.8	106.3	106.0	106.5
380	4.5	11.25	16	108	112.4	109.3	111.1	111.1
381	4.5	11.25	17.5	110	112.1	113.0	114.9	116.1
382	4.5	11.25	16.5	112	112.3	113.2	112.4	112.8
383	4.5	11.25	18.5	112	114.0	112.7	113.1	113.1
384	5	12.50	16	118	120.0	114.0	118.5	118.1
385	5	12.50	16.5	120	119.9	117.9	120.1	119.6
386	5	12.50	18.5	120	122.1	119.2	121.0	117.5
387	5	12.50	17.5	120	119.7	118.5	123.3	122.5

Note: P_{out}^{exp} is the experimentally found output power and $P_{out}^{(30;2)}$, $P_{out}^{(40;2)}$, $P_{out}^{(30;3)}$, and $P_{out}^{(40;3)}$ are the output powers calculated according to the models (30;2), (40;2), (30;3), and (40;3), respectively.

6.2. Prediction of the results of future experiments

By analogy with Subsection 6.1, MARS models can also be used to predict the results of new experiments. Our purpose was to predict the characteristics of copper bromide lasers with increased output power. To this end, we will set (taking into account the behaviour of the main predictors in the intervals where P_{out} increases) new sets of characteristics and calculate the corresponding approximations for P_{out}. The thus obtained predictions for ten chosen sets of parameters, denoted as v_{pr}, are listed in Table 4.

7. Physical interpretation of the simulation results

When constructing models for calculating the output power P_{out}, we used ten independent variables. Nine of them are physical, and only the variable $P_L = P_{in}/L$ (with allowance for 50% loss) is derivative. As was noted in Section 5, in the second- and third-order models for calculating the output power of copper bromide lasers, only the following six input parameters are significant: P_{in}, C, P_{rf}, D_r, p_{H_2}, P_L. Of prime importance is the supplied electric power P_{in} (almost 100 relative units), which is in good correspondence with the real

Table 4. Results predicted based on 387 real observations using four MARS models for ten planned experiments ($P_{rf} = 17.5$ kHz, $C = 1.3$ nF).

v_{pr}	D	D_r	L	P_{in}	P_L	p_{H_2}	p_{Ne}	T_r	$P_{out}^{(30;2)}$	$P_{out}^{(40;2)}$	$P_{out}^{(30;3)}$	$P_{out}^{(40;3)}$
1	60	60	210	5.1	12.14	0.6	20	490	125.0	124.1	127.1	127.8
2	68	65	220	5.2	11.82	0.6	20	500	132.4	131.5	130.8	133.0
3	70	68	225	5.25	11.67	0.6	20	500	136.4	135.6	132.7	135.6
4	75	73	230	5.3	11.52	0.5	20	500	144.7	142.6	134.5	138.2
5	70	70	240	5.5	11.46	0.5	20	500	147.9	145.8	139.9	144.7
6	70	70	240	5.6	11.67	0.5	20	500	149.4	146.9	141.5	145.9
7	70	68	240	5.7	11.88	0.5	21	500	149.4	146.7	143.1	147.0
8	75	73	240	5.5	11.46	0.5	21	500	150.0	147.8	139.9	144.7
9	70	70	240	5.7	11.88	0.5	21	500	150.8	148.0	143.1	147.0
10	75	75	240	5.7	11.88	0.5	21	500	154.3	151.3	143.1	147.0

Note: $P_{out}^{(30;2)}$, $P_{out}^{(40;2)}$, $P_{out}^{(30;3)}$, and $P_{out}^{(40;3)}$ are the output powers calculated according to the models (30;2), (40;2), (30;3), and (40;3), respectively.

experiment. The contribution of the capacitor battery capacitance C and the electric pulse repetition frequency P_{rf} to the model is 20–35 rel. units, while the contribution of the other variables is 10–15 rel. units. These six parameters affect significantly the average output laser power, because they set the electric field distribution, the electron energy, and the temperature profile of ionised gas. All these factors affect the occupation of upper laser levels and, therefore, the lasing power P_{out}.

The variable P_L is of particular importance for designing the laser tube. It must be taken into account to obtain good results in both the MARS analysis and parametric models [3–7]. The predicted results in Table 4 show a decrease in P_L. This means that L should increase more rapidly than P_{in} to reduce the ratio $P_L = P_{in}/L$. Physically, this is explained by the fact that an increase in the interelectrode distance L leads to redistribution of the input electric power P_{in} between the electrodes and in the active volume of positive gas-discharge column; this redistribution increases the output power and lasing efficiency.

Another important parameter for designing lasers is the specific power $P_V = P_{in}/V$ (in W cm^{-3}); i.e., the power per unit active volume V in the laser tube, with allowance for 50% loss. For the last three rows in Table 3 (P_{out} = 120 W), P_V = 0.47 W cm^{-3}. For the ten predicted sets of variables (ν_{pr}) in Table 4, the P_V value decreases with an increase in the set number. The calculations show that the corresponding P_V values are smaller than 0.47 W cm^{-3} by 30%–35%. This deviation can be explained by higher input powers for the laser under study. With allowance for the results obtained, a specific input power P_V = 0.3 W cm^{-3} can be recommended for designing future lasers. Using this value, one can decrease the thermochemical degradation of the laser tube and active operating materials, increase the service life, and reduce the decrease in the average laser power in the tube during its operation.

8. Conclusions

Statistical simulation of the dependence of the output laser power on ten input variables was performed for copper bromide lasers using the predictive MARS technique. Partially linear and partially nonlinear MARS models were constructed based on a large amount of known experimental data to yield a very good approximation to the initial data sets. Six main variables were selected for calculating the output laser power. The models obtained were used both to calculate the parameters of existing lasers and predict the characteristics of future lasers. The models constructed and the predictions were physically interpreted. The approach developed and the results obtained can be used to plan future experiments.

Acknowledgements. This study was supported by the NPD foundation of Paisii Hilendarski University of Plovdiv (Project No. NI11-FMI-004).

References

1. *Entsiklopediya nizkotemperaturnoi plazmy. Seriya B. Tom XI-4. Gazovye i plazmennye lazery* (Encyclopedia of Low-Temperature Plasma, Series B, Vol. XI-4: Gas and Plasma Lasers). Ed. by S.I. Yakovlenko (Moscow: Fizmatlit, 2005).
2. Boichenko A.M., Evtushenko G.S., Zhdaneev O.V., Yakovlenko S.I. *Kvantovaya Elektron.*, **33**, 1047 (2003) [*Quantum Electron.*, **33**, 1047 (2003)].
3. Iliev I.P., Gocheva-Ilieva S.G., Astadzhanov D.N., Denev N.P., Sabotinov N.V. *Kvantovaya Elektron.*, **38**, 436 (2008) [*Quantum Electron.*, **38**, 436 (2008)].
4. Iliev I.P., Gocheva-Ilieva S.G., Astadjov D.N., Denev N.P., Sabotinov N.V. *Opt. Laser Technol.*, **40**, 641 (2008).
5. Gocheva-Ilieva S.G., Iliev I.P. *Math. Probl. Eng.*, **2010**, Article ID 697687 (2010).
6. Gocheva-Ilieva S.G., Iliev I.P. *Proc. 19th Int. Conf. on Computational Statistics* (*COMPSTAT'2010*) (Paris: Physica-Verlag, Springer_ebook, 2010) pp 1063–1070.
7. Gocheva-Ilieva S.G., Iliev I.P. *Statistical Models of Characteristics of Metal Vapor Lasers* (New York: Nova Science Publ. Inc., 2011).
8. Friedman J.H. *Ann. Stat.*, **19**, 1 (1991).
9. Astadjov D.N., Vuchkov N.K., Sabotinov N.V. *IEEE J. Quantum Electron.*, **24**, 1927 (1988).
10. Vuchkov N.K., Astadjov D.N., Sabotinov N.V. *Opt. Quantum Electron.*, **23**, S549 (1991).
11. Astadjov D.N., Dimitrov K.D., Little C.E., Sabotinov N.V. *IEEE J. Quantum Electron.*, **30**, 1358 (1994).
12. Dimitrov K.D., Sabotinov N.V. *Proc. SPIE Int. Soc. Opt. Eng.*, **3052**, 126 (1996).
13. Astadjov D.N., Dimitrov K.D., Jones D.R., Kirkov V.K., Little L., Little C.E., Sabotinov N.V., Vuchkov N.K. *Opt. Commun.*, **135**, 289 (1997).
14. Astadjov D.N., Dimitrov K.D., Jones D.R., Kirkov V.K., Little C.E., Sabotinov N.V., Vuchkov N.K. *IEEE J. Quantum Electron.*, **33**, 705 (1997).
15. *NATO contract SfP*, 97 2685 (2000).
16. Stoilov V.M., Astadjov D.N., Vuchkov N.K., Sabotinov N.V. *Opt. Quantum Electron.*, **32**, 1209 (2000).
17. Denev N.P., Astadjov D.N., Sabotinov N.V. *Proc. IV Int. Symp. on Laser Technologies and Lasers 2005* (Plovdiv, 2006) p. 153.
18. http://salford-systems.com/products/mars/overview.html.
19. *MARS 3.0 Technical User's Guide, Salford Systems* (San Diego, California, 2011).
20. Craven P., Wahba G. *Numer. Math.*, **31**, 377 (1979).